In Situ IR Study of Transient CO_2 Reforming of CH_4 over Rh/Al_2O_3

Robert W. Stevens, Jr. and Steven S. C. Chuang*

The University of Akron, Akron, Ohio 44325-3906

Received: September 15, 2003; In Final Form: October 24, 2003

The CO_2-CH_4 reaction on Rh/Al_2O_3 was studied by in situ infrared spectroscopy coupled with pulse and step transient techniques. Steady-state isotopic ^{13}CO transient studies at 773 K and 0.1 MPa show that the formation of gaseous $^{13}CO_2$ closely follows that of linear ^{13}CO, indicating that linear CO is an active adsorbate. Pulsing CH_4 into CO_2 flow and step switching from He to CO_2/CH_4 flow showed that the formation of H_2 led that of CO, revealing that the first step of the reaction sequence is the decomposition of CH_4 into $*CH_x$ species and hydrogen. Hydrogen activated adsorbed CO_2 to produce linear CO. The linear CO was found to be the major species on Rh/Al_2O_3 during the reaction by in situ infrared spectroscopy. The accumulation of the linear CO on Rh^0 sites revealed that the surface of Rh crystallites on Al_2O_3 remained in a reduced state throughout the study. The O_2 pulse into CO_2/CH_4 resulted in (i) a total oxidation of CH_4 to CO_2 and H_2O and then (ii) a net increase in the formation of the desired products, CO/H_2, at a ratio of 1:1, revealing the promotion of the CO_2-CH_4 reaction. These are the first reported results on the enhancement of the CO and H_2 formation rate via the pulse addition of oxygen into the CO_2-CH_4 reaction. The difference in product formation can be explained by two different types of adsorbed oxygen: one responsible for total oxidation and the other responsible for partial oxidation. The net increase in CO and H_2 formation from the O_2 pulse further suggests that combining mixed reforming of CH_4 with CO_2/O_2 and selective poisoning of the total oxidation sites would enhance the selectivity and rate of CO/H_2 formation.

Introduction

The CO_2 reforming of methane reaction produces synthesis gas, which is useful as a feedstock for many important industrial processes: methanol production, the Fischer−Tropsch process, and fuel cell processes. This reaction is attractive due to its low reactant cost and low H_2/CO product ratio, which is favorable for the Fischer−Tropsch synthesis.[1] However, this reaction is highly endothermic ($\Delta H° = 59.1$ kcal/mol) and requires temperatures of 1000 K or higher to achieve significant conversion. Lowering operating temperature, enhancing reaction rate, increasing the selectivity toward desired products, and improving deactivation characteristics will significantly increase the overall economics of the CO_2-CH_4 reforming process.

Rh,[2−10] Ru,[4,11] Pd,[12,13] Pt,[14,15] and Ni[9,16−18] have all been shown as active catalysts for the CO_2-CH_4 reforming reaction. While Ni is significantly cheaper than precious metals (i.e., approximately 22 times cheaper[19] than Rh on a cost per atom basis), it suffers from deactivation due to coking formed from surface carbon. Carbon deposits may be formed from both CH_4 decomposition and CO disproportionation ($2CO + * \rightarrow *C + CO_2$, where "*" is an active site).[20] Many studies have been focused on reducing this coke formation on the Ni catalysts; basic supports such as MgO or promoters such as CaO have shown promise in its suppression.[17,18] Although the noble metals are expensive, they possess an ability to resist the formation of coke during the CO_2-CH_4 reforming reaction.[10,20,21] Rh has been demonstrated to possess one of the highest activities in terms of turnover frequency, TOF.[20]

The formation of CO and H_2 from the reforming reaction on the Rh catalyst involves (i) the breaking of a C−O bond in CO_2 and C−H bonds in CH_4 and (ii) the interactions and reactions of the species resulting from these bond-breaking processes. The key issues regarding the reforming mechanism are determination of (i) the reaction pathway, (ii) the rate-limiting step, and (iii) the nature of active sites. A fundamental understanding of the reaction mechanism may guide catalyst design and operating condition optimization to control the reaction pathways, which may lead to enhanced activity and/or selectivity.

The objective of this study is to investigate the mechanism of the CO_2-CH_4 reaction on Rh by in situ infrared (IR) spectroscopy coupled with mass spectrometry (MS) analyses. The key features of this technique include (i) simultaneous measurement of the dynamics of adsorbed species and product formation, (ii) use of $^{13}CO_2$ as a tracer, and (iii) use of O_2 as either a promoter or poison toward product formation. The use of a $^{13}CO_2$ isotopic tracer allows determination of the residence time of intermediates for conversion of CO_2 to CO. The addition of O_2 may perturb the dynamics of adsorbates and oxidation states. The combined use of $^{13}CO_2$ isotopic tracing as well as CH_4 and O_2 pulsing can provide a wealth of information pertaining to the reaction dynamics on the catalyst surface, which can lead to elucidation of the CO_2-CH_4 reaction mechanism.

Experimental Section

Catalyst Preparation and Characterization. The 2 wt % Rh/Al_2O_3 catalyst was prepared by incipient wetness impregnation using an aqueous solution of $RhCl_3 \cdot 2H_2O$ (Alfa Chemicals) onto γ-Al_2O_3 (Alfa Chemicals, 100 m^2/g). The catalyst was dried overnight in air at room temperature and calcined in flowing air at 723 K for 6 h. It was then reduced in flowing hydrogen at 723 K for an additional 6 h. The catalyst was characterized

* Corresponding author. Fax: (330) 972-5856. E-mail: schuang@uakron.edu.

10.1021/jp0367530 CCC: $27.50
Published on Web 12/10/2003

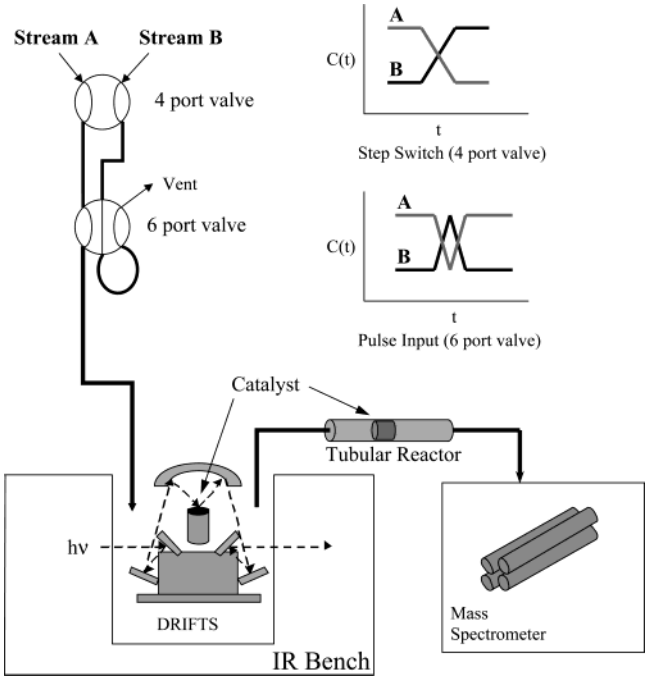

Figure 1. Experimental apparatus.

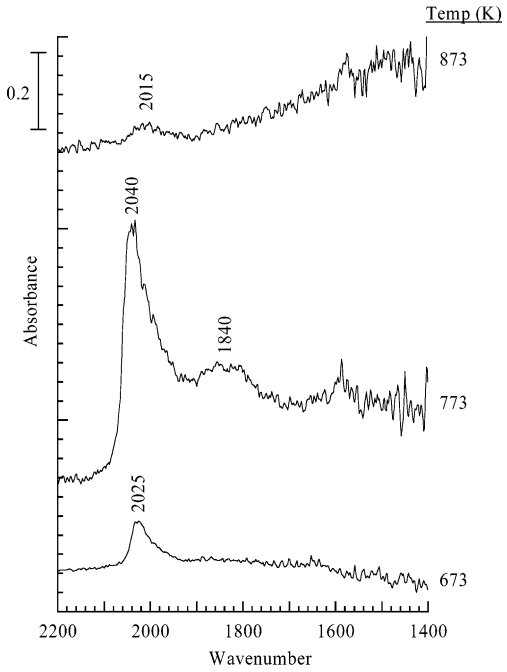

Figure 2. DRIFTS spectra of Rh/Al_2O_3 surface under steady-state CO_2/CH_4/He flow at (a) 673, (b) 773, and (c) 873 K. Conditions: 1 atm; CO_2/CH_4/He flow = 3/3/34 sccm.

TABLE 1: Conversion and Rate Summary for CO_2 Reforming of CH_4 Reaction as a Function of Temperature

	conversion (%)		rate of formation, TOF (s^{-1})	
temp (K)	CH_4	CO_2	CO	H_2
673	4.5	13.1	0.03	0.03
773	8.3	24.3	0.07	0.04
873	21.8	47.9	0.16	0.10
973	67.9	76.1	0.35	0.45

by H_2 chemisorption; the average particle size was determined to be 52 Å, which corresponded to a dispersion of 17.6%. A FEI-TACNAI 12 transmission electron microscope (TEM) was used to compare the catalyst surface before and after the reaction studies (see TEM Analysis). Due to the limited resolution of the TEM as well as its localized analysis, the TEM was not used for particle size measurement.

Experimental Apparatus. The experimental apparatus is shown in Figure 1; it has been described in detail elsewhere and therefore will only be discussed briefly here.[22] For each experiment, a total of 120 mg of catalyst powder was used. Approximately 20 mg of Rh/Al_2O_3 was placed into a DRIFTS (diffuse reflectance infrared Fourier transform spectroscopy; Spectra-Tech Model 0030-102) reactor while the remaining 100 mg was charged to a tubular reactor (connected in series to the effluent of the DRIFTS) to increase the conversion of reactants. DRIFTS was used for this study due to its ability to reach higher temperatures than that of the transmission IR cell described in the above reference. The DRIFTS reactor resided in a Nicolet Magna 560 infrared (IR) spectrophotometer bench; all spectra were collected at a resolution of 4 cm^{-1} with 32 co-added scans. The effluent of the DRIFTS−tubular reactor was monitored via a Balzers/Pfeiffer Prisma QMS 200 mass spectrometer (MS), allowing the determination of reactant conversions, product selectivity, and rate data. Separate temperature control systems existed on each of the reactors, allowing for ease of maintaining equal temperature between the two reactors at all times.

CH_4 (Praxair, 99.97%), CO_2 (Praxair, 99.998%), He (Praxair, 99.999%), and O_2 (Praxair, 99.999%) flows to the reactor were controlled via Brooks 5850 mass flow controllers at a total flow rate of 40 cm^3/min and a pressure of 0.1 MPa. Feed gas composition differed in each experiment and will be specified in their respective figure captions. Prior to each experiment, the catalyst was reduced in situ in H_2 flow for 1.5 h at 773 K and subsequently flushed with He flow.

Transient Studies. The inset of Figure 1 illustrates two transient techniques: a step switch and a pulse input. Both techniques perturbed the reaction and produced transient responses of the reactants, products, and adsorbates for elucidation of the reaction mechanism. The four-port valve allows for a step switch, whereas the six-port valve allows introduction of a pulse of known volume and concentration of one reactant into the flowing stream of another reactant. A step switch provides a rapid replacement of one flow stream with another, in which flow rates of the two streams are identical. The isotopic transient was conducted by step switching $^{12}CO_2$ to $^{13}CO_2$ flow while maintaining a constant CH_4 flow. An example of the pulse technique includes introduction of 1 cm^3 of O_2 into flowing CH_4/CO_2 and observing the dynamic behavior that follows. All of these observations provide insight into the reaction mechanism.

Results

Reaction Conditions. Figure 2 depicts IR spectra taken during the steady-state CO_2-CH_4 reaction over Rh/Al_2O_3 at 673, 773, and 873 K. Table 1 lists reactant conversions and TOF as a function of temperature. The rates obtained are in agreement with those reported in the literature.[20] At 673 K, the major species observed by IR is linear CO at 2025 cm^{-1}. Increasing the reactor temperature to 773 K led to a higher concentration of linear CO and formation of bridged CO on the catalyst surface as well as increased reactant conversions. Further increase in temperature led to a higher conversion, but with a decrease in adsorbate intensity.

The intensity of the adsorbed species depends on its formation and conversion rates. As the temperature is increased from 673 to 773 K, the formation rate of linear CO increased faster than its desorption rate, creating a larger amount of accumulated CO

on the surface of the catalyst. Increasing temperature to 873 K and higher resulted in a further increase in the reactant conversions as well as the rate of consumption of adsorbed CO. Thus, the intensity of adsorbed CO is smaller at 873 K than at 773 K. Therefore, 773 K was selected as the temperature to conduct all of the transient studies. This temperature gave a balance between the reactivity of the catalyst and the concentration of adsorbed intermediates, which provided a clear variation in the concentration of reactants, products, and adsorbed intermediates during the transient studies.

It should be noted that the adsorbed CO shifted upward in wavenumber as its intensity increased. This shift confirms the assignment of the 2015−2040 cm^{-1} band shown in Figure 2 to linear CO instead of adsorbed CHO species. Yates and Cavanagh have shown that the wavenumber of the adsorbed CHO does not vary with its intensity.[23] The shift in adsorbed CO wavenumber can be attributed to a dipole−dipole interaction between the linear CO on the surface of Rh.[24,25] If the supported Rh is highly dispersed, however, then adsorbed CO species would not interact with one another and thus would not give rise to a wavenumber shift. The obvious shift in position of linear CO with increasing intensity in Figure 2 suggests that the CO adsorption sites of the supported Rh are in close proximity (i.e., large particle size/low dispersion). The average particle size of our catalyst was determined to be 52 Å by H_2 chemisorption (17.6% dispersion).

Steady-State $^{13}CO_2$ Isotopic Transient Study. Figure 3 illustrates the normalized MS profiles of CO and CO_2 resulting from a step switch from $^{12}CO_2$ to $^{13}CO_2$ while maintaining constant CH_4/He flow (i.e., step switch from $^{12}CO_2/CH_4$/He to $^{13}CO_2/CH_4$/He) at 773 K. To closely discern the lead−lag relationship between CO and CO_2 as well as their isotopic counterparts, the MS profiles were normalized using the formula $F(t) = [C(t) - C_0]/[C_\infty - C_0]$, where $F(t)$ represents normalized intensity as a function of time, $C(t)$ is the intensity of an MS profile at a given time, and C_0/C_∞ are the initial/final intensities before/after the step switch. The IR results of the gaseous and adsorbed species taken during the step switch are illustrated in Figure 4. The $^{12}CO_2$ to $^{13}CO_2$ step switch led to (i) a decrease in adsorbed CO (^{12}CO) at 2040 cm^{-1} with a concurrent increase in adsorbed ^{13}CO intensity at 2001 cm^{-1}, shown in Figure 4, and (ii) decay of gaseous ^{12}CO and evolution of gaseous ^{13}CO. The parallel decrease in gaseous $^{12}CO_2$/linear ^{12}CO/gaseous ^{12}CO along with the parallel increase in gaseous $^{13}CO_2$/linear ^{13}CO/gaseous ^{13}CO revealed that the isotope-labeled species replaced the nonlabeled species in the reaction pathway: CO_2 → linear CO → CO. The replacement process propagated through the reaction intermediates and finally reached the reaction products.[26,27] This observation confirms that the linear CO is an active adsorbate which leads to the formation of gaseous CO.

The average residence time of transient intermediates leading to the gaseous product CO, τ_{CO}, can be calculated by subtracting the residence time of the normalized CO_2 response from the residence time of the normalized CO response.[28,29] Subtraction of the $^{13}CO_2$ response is required because the CO_2 response curve is an accurate representation of the flow pattern as evidenced by our previous study (i.e., analogous to a tracer response).[30] This residence time, τ_{CO}, for the intermediates was determined to be 1.6 s. The CO coverage, θ_{CO} (moles of adsorbed CO per moles of surface Rh), can be determined from TOF $= k\theta = \theta/\tau$, where k (min^{-1}) is the rate constant. θ_{CO} was found to be 0.112 using the above equation along with the TOF for CO at 773 K. Efstathiou et al. used a steady-state isotopic

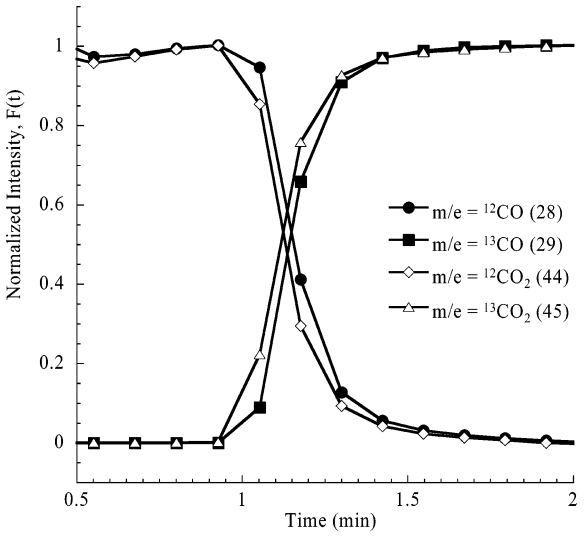

Figure 3. Normalized rates of formation, $F(t)$, from an isotopic step switch ($^{12}CO_2/CH_4$/He → $^{13}CO_2/CH_4$/He) illustrating the lead−lag relationship. Conditions: 1 atm; 773 K; CO_2/CH_4/He flow = 3/3/34 sccm.

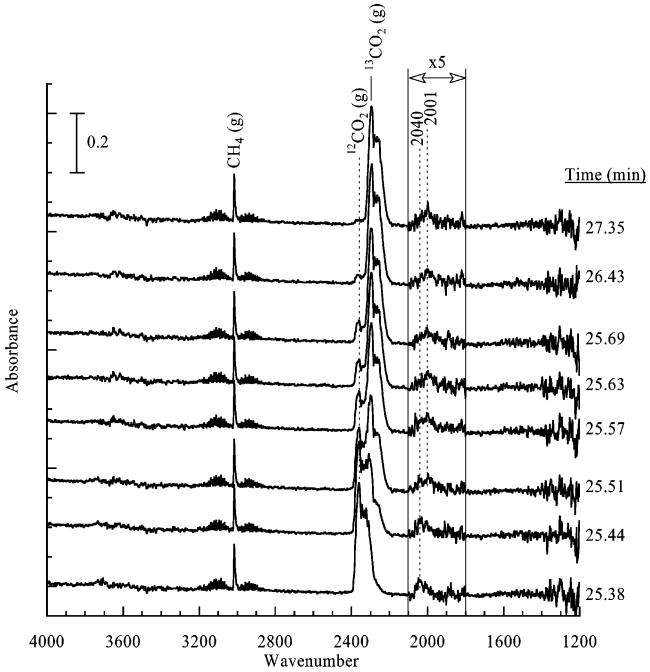

Figure 4. DRIFTS analysis of the step switch from $^{12}CO_2/CH_4$/He to $^{13}CO_2/CH_4$/He at 773 K. Ratio of CH_4:CO_2 flow = 1:1. Times indicated are relative to the time of the step switch. Conditions: 1 atm; 773 K; CO_2/CH_4/He flow = 3/3/34 sccm.

tracing technique and temperature-programmed oxidation to determine the surface coverage of carbon-containing (θ_C) and oxygen-containing (θ_O) intermediates leading to the formation of CO over Rh/Al_2O_3 during CO_2-CH_4 reforming at 623 K to be 0.2 and 0.02, respectively.[3] Similarly, θ_{CO} has been determined to be 0.57 for CO hydrogenation on Rh/SiO_2 at 513 K ethylene hydroformylation on Rh.[28] Biloen suggested that θ_{CO} is an intrinsic property of the catalyst and represents only the amount of surface sites occupied by CO under steady-state conditions.[31] It has been demonstrated that θ_{CO} varies with the partial pressure of reactants.[32] θ_{CO} does not reflect the total number of surface sites available; it is a function of individual rates of formation, consumption, and desorption which is strongly dependent on temperature and reactant partial pressures.

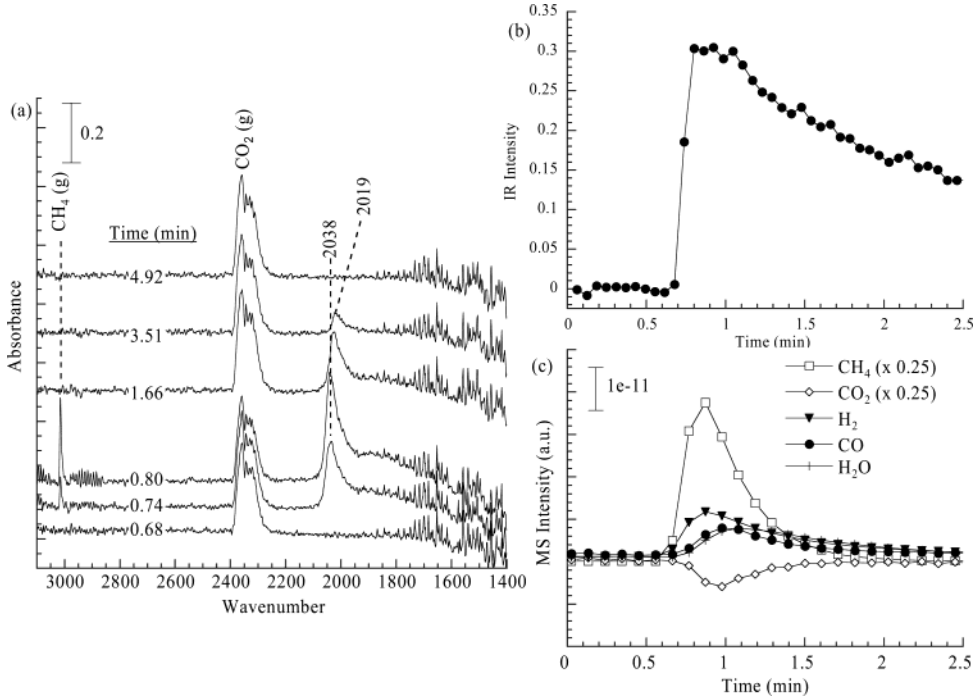

Figure 5. CH_4 pulse into steady-state CO_2/He flow over Rh/Al_2O_3 at 773 K as analyzed by (a) DRIFTS, (b) IR intensity vs time of adsorbed CO, and (c) mass spectrometry. Times indicated are relative to the time of CH_4 admission. Conditions: 1 atm; 773 K; CO_2/He flow = 3/37 sccm; CH_4 pulse = 1 cm^3.

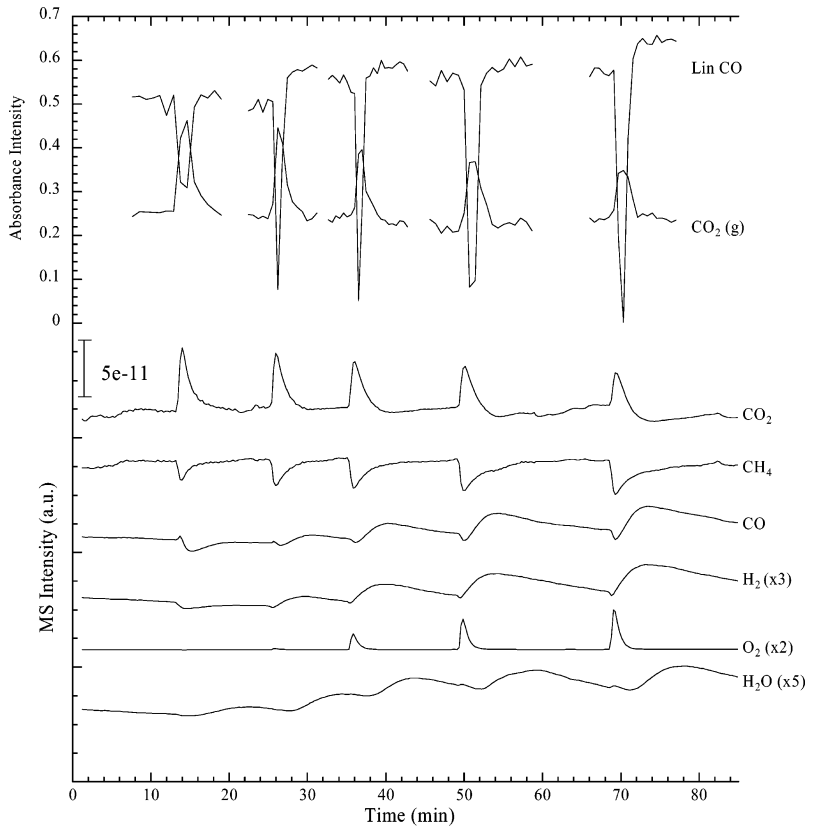

Figure 6. MS analysis of the O_2 pulsing series into CO_2/CH_4/He flow over Rh/Al_2O_3 at 773 K. Conditions: 1 atm; 773 K; CO_2/CH_4/He flow = 3/3/34 sccm; O_2 pulse = 1 cm^3.

CH_4 Pulsing into CO_2 Flow. Figure 5 shows IR and MS analyses during a 1 cm^3 CH_4 pulse into steady-state CO_2 flow (10% in He) at 773 K. Under the steady-state CO_2 flow at this temperature, no adsorbates were initially present on the surface, as shown by the first spectrum of Figure 5a. As the catalyst was exposed to the CH_4 pulse, linear CO at 2038 cm^{-1} formed rapidly. This was coupled with a formation of products H_2 and CO, as illustrated in Figure 5c. The formation of H_2 led that of CO and H_2O, suggesting that formation and desorption of H_2 is facile. Due to the adsorption and slow desorption of H_2O on the transportation line, the H_2O response lagged behind those of other gaseous species.

The increasing and decreasing intensity of linear CO on the surface of the catalyst followed the same trends of CO

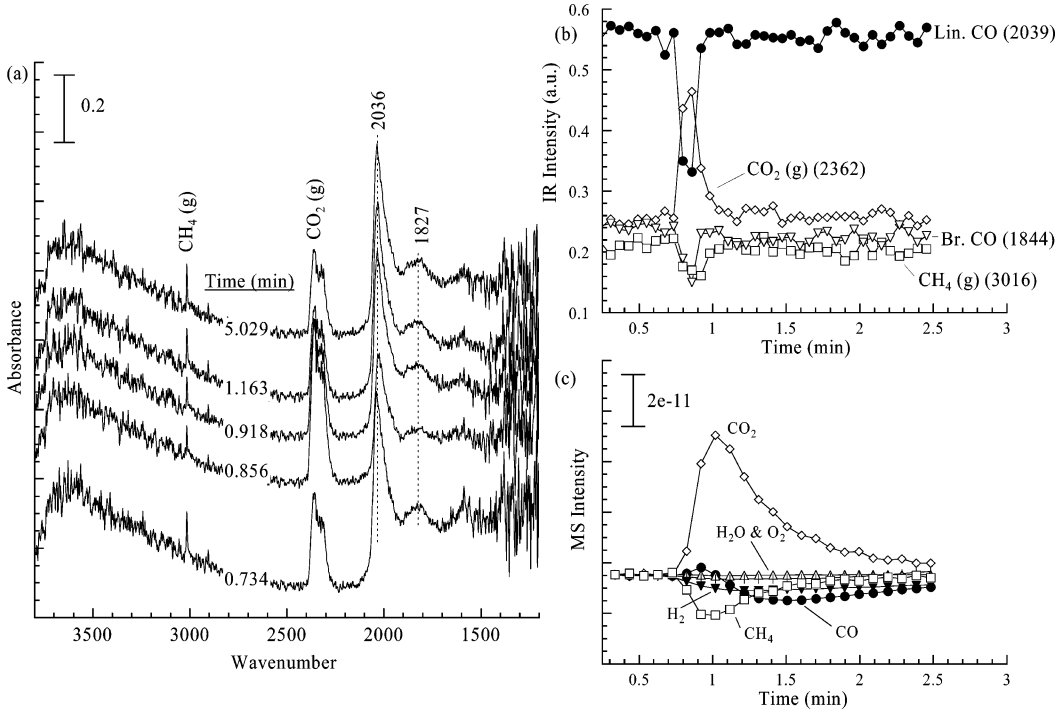

Figure 7. First O_2 pulse into steady-state CH_4/CO_2/He flow over Rh/Al_2O_3 at 773 K as analyzed by (a) DRIFTS, (b) intensities vs time of selected species, and (c) mass spectrometry. Times indicated are relative to the time of O_2 admission. Conditions: 1 atm; 773 K; CO_2/CH_4/He flow = 3/3/34 sccm; O_2 pulse = 1 cm^3.

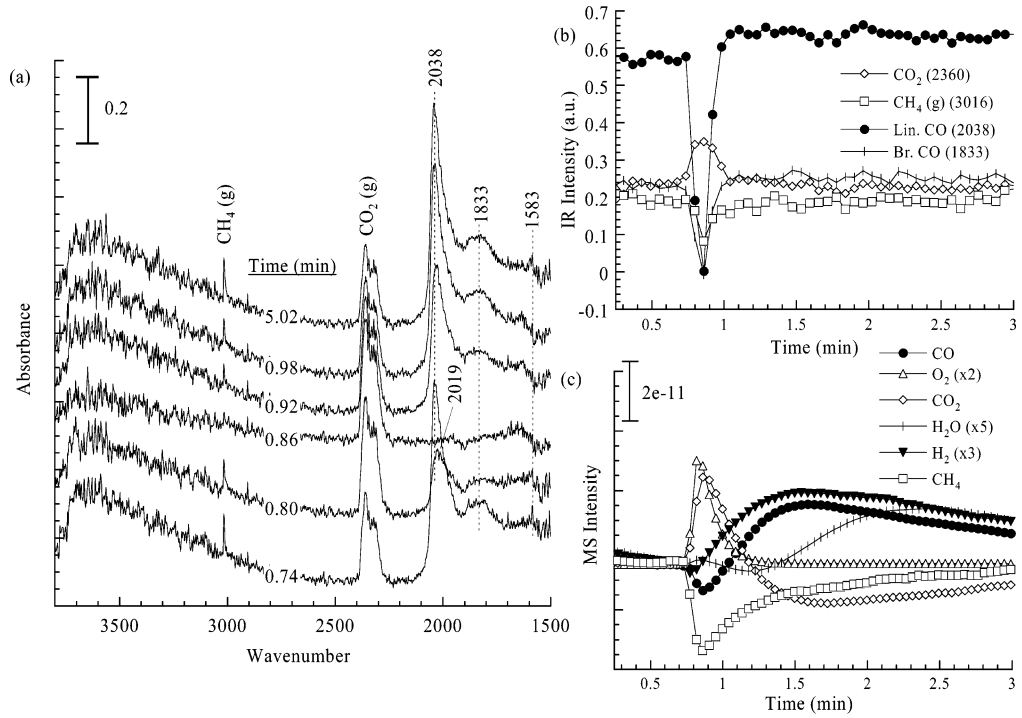

Figure 8. Fifth O_2 pulse into steady-state CH_4/CO_2/He flow over Rh/Al_2O_3 at 773 K as analyzed by (a) DRIFTS, (b) intensities vs time of selected species, and (c) mass spectrometry. Times indicated are relative to the time of O_2 admission. Conditions: 1 atm; 773 K; CO_2/CH_4/He flow = 3/3/34 sccm; O_2 pulse = 1 cm^3.

concentration in the reactor effluent, further confirming that linear CO (Rh^0-CO) is an active adsorbate during the CO_2-CH_4 reaction. The shift in the wavenumber of adsorbed CO with its intensity from 2038 to 2019 cm^{-1}, indicative of dipole−dipole interactions, is consistent with the observations depicted in Figure 2. Although the wavenumber of Rh−CHO species (Rh carbonyl hydride) falls in the same range as that of linear CO,[23] the invariance of the Rh−CHO wavenumber with its intensity as well as the downward shift of the 2038−2019 cm^{-1} bands with their intensities ruled out the assignment of the 2038−2019 cm^{-1} band to a Rh−CHO species.

O_2 Pulsing into CO_2/CH_4 Flow. The objective of the O_2 pulse is to probe the role of adsorbed oxygen in the formation of CO/H_2. Figure 6 summarizes the results of O_2 pulsing into steady-state CO_2/CH_4 flow over Rh/Al_2O_3 at 773 K as analyzed by infrared spectroscopy and mass spectrometry. The intensities of the MS profiles prior to the O_2 pulsing represent the steady-state concentration profiles of the reactants/products, indicating

the occurrence of the steady-state CO_2-CH_4 reaction. The first pulse of O_2 was completely consumed, as evidenced by the flat O_2 profile, and caused formation of only CO_2 and H_2O; the formation of products, CO and H_2, was decreased by the pulse as indicated by the negative peaks within their profiles, suggesting that the pulse inhibited the desired reaction and caused complete combustion of CH_4 to occur.

Exposure of the catalyst to the second pulse of O_2 led to an initial decrease in H_2 and CO formation followed by enhanced formation of H_2 and CO, as shown by the increased intensities of their MS profiles. Subsequent pulses of O_2 revealed the existence of a trend that became more apparent with each pulse: (i) greater formation of H_2 and CO products, (ii) lesser formation of CO_2, (iii) greater enhancement of CH_4 conversion, and (iv) lesser consumption of O_2. The comparison of the enhanced amount of CO and H_2 produced in the subsequent pulses shows that the ratio of CO to H_2 is approximately unity, suggesting that the additional CO and H_2 produced resulted from the CO_2-CH_4 reaction.

Figure 7 illustrates the details of the first O_2 pulse at 773 K. Steady-state CO_2/CH_4 flow over the catalyst at 773 K led to the formation of linear CO at 2036 cm^{-1} and bridged CO at 1827 cm^{-1} as shown in the first spectrum of Figure 7a. The variation in IR intensity with time is plotted in Figure 7b with MS profiles in Figure 7c. Figure 7a,b shows that the exposure of the catalyst to the O_2 pulse resulted in approximately 50% removal of the adsorbed CO in the form of CO_2; it is also illustrated that CO_2 was evolved as a result of the O_2 pulse whereas the formation of the desired products, i.e., CO and H_2, was decreased. Shortly after the O_2 pulse, product formation as well as adsorbate intensities returned to their respective steady-state levels. As the O_2 pulse travels through the transport lines (i.e., tubing) of the experimental system, it broadens due to axial dispersion, thus being more diffuse by the time it reaches the MS as compared to that of the IR.[33] For this reason, the time scale of the MS profile has been adjusted to match that of the IR by correlating relative maxima and minima observed from each instrument. This synchronization was performed on all similar figures presented.

Figure 8 depicts IR and MS analyses during the addition of the fifth O_2 pulse into CO_2/CH_4 flow over the catalyst at 773 K. In addition to the events occurring during the first pulse (Figure 7), the fifth pulse resulted in (i) removal of adsorbed linear and bridged CO from the surface in the form of CO_2 as evidenced by the decrease in the linear CO band and concurrent increase in the CO_2 band, (ii) a temporary decrease in the broad band in the $-OH$ stretch region at $\sim$3600 cm^{-1} and the formate band at 1583 cm^{-1}, and (iii) an increase in the CH_4 consumption as evidenced by the decrease in CH_4 at 3016 cm^{-1}. Following the initial evolution of CO_2, the products CO and H_2 were produced at an enhanced rate which lasted for several minutes, after which the reactant conversion and product formation rates returned to steady-state levels.

The lead−lag relationship of adsorbed species and products from the O_2 pulse shown in Figure 8 reveals the sequence of reactant conversion, reaction intermediates, and product formation. The response of reactants/products may be divided into two stages.

Stage I: The initial increase in CO_2 formation, as evidenced by its IR and MS intensities, indicates occurrence of CH_4 oxidation to produce CO_2 and H_2O as well as oxidation of the adsorbed CO species. The H_2O MS profile is not initially observed, in part due to its inherent transport lag resulting from adsorption/desorption with the walls of the transport lines.

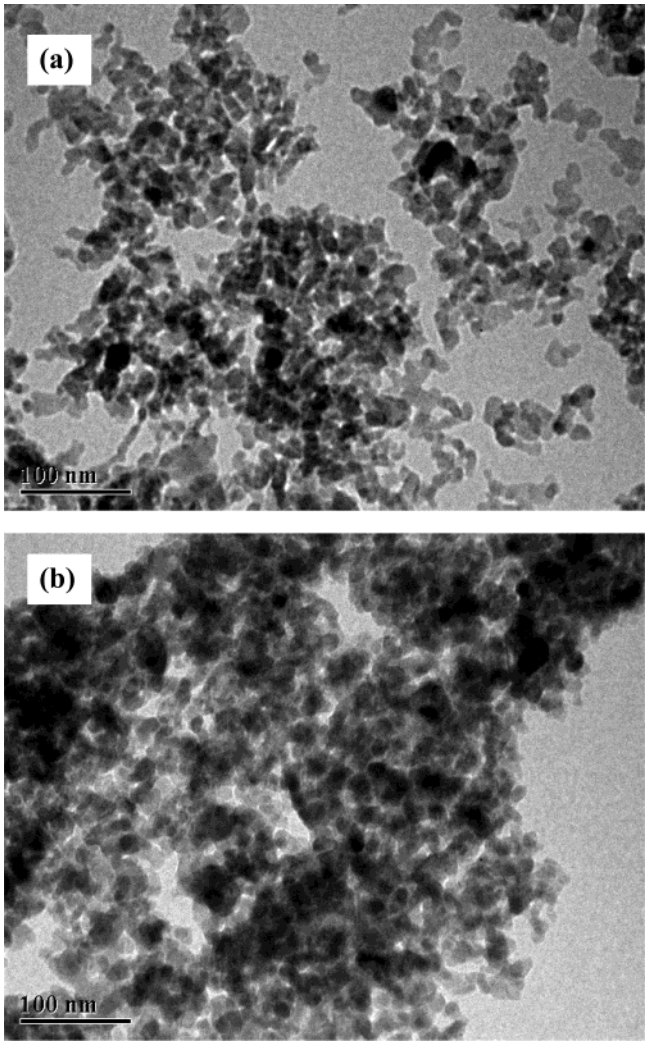

Figure 9. TEM images of (a) fresh Rh/Al_2O_3 catalyst and (b) used Rh/Al_2O_3 catalyst (i.e., after reaction studies).

Stage II: Following the peak of CO_2, H_2 and then CO concentrations began increasing, as evidenced by the rise in their respective MS profiles. Integrating the area of H_2 and CO profiles and multiplying the area with their respective response factors allowed us to quantify the increased amounts of H_2 and CO resulting from the O_2 pulse. The ratio of the increased H_2 to CO was found to be 1:1, indicating that the increased H_2 and CO were produced from the CO_2-CH_4 reaction ($CO_2 + CH_4 \rightarrow 2CO + 2H_2$; $H_2/CO = 1$) rather than that of partial oxidation ($CH_4 + (1/2)O_2 \rightarrow CO + 2H_2$; $H_2/CO = 2$). Enhancement of the CO_2-CH_4 reaction is further evidenced by the simultaneous increases in H_2 and CO and decreases in CO_2 and CH_4 occurring between 1.3 and 5 min during the O_2 pulse shown in Figures 6 and 8; if enhancement was due to the partial oxidation reaction, it would be expected that CO_2 conversion would decrease or remain constant rather than increase.

H_2O produced from the CO_2-CH_4 reaction can further undergo the water-gas shift (WGS) reaction, $H_2O + CO \rightarrow H_2 + CO_2$. We have recently further confirmed the occurrence of the water-gas shift reaction by addition of D_2O into the CH_4-CO_2 stream.[30] The occurrence of the WGS reaction could contribute to a slightly higher ratio for the increased H_2/CO than its stoichiometric ratio during the O_2 pulse.

TEM Analysis. Figure 9 illustrates the transmission electron micrographs of (a) fresh Rh/Al_2O_3 and (b) used Rh/Al_2O_3

following reaction study. Dark spots within the image represent rhodium, whereas the lighter spots represent the Al_2O_3 support. It is important to note that thick areas of support can appear to be dark and should not be misconstrued as rhodium particles. Initially, the Rh particles are well distributed throughout the support as suggested by the scatter of darkened areas in Figure 9a. While the resolution of the TEM does not allow observation of particles below ~40 Å, many observable Rh particles are in the range of 50−90 Å. Following the CO_2/CH_4 reaction studies (Figure 9b), there is no evidence of particle size growth (i.e., agglomeration). The indifference in particle size between the before and after TEM photographs suggests that the catalyst was unchanged during the series of experiments.

SO_2 Poisoning Study. Exposure of the Rh catalyst to flowing SO_2 at 773 K led to the deactivation of the catalyst (results not shown); conversions of CO_2 and CH_4 as well as formation of CO and H_2 were determined to be negligible following the treatment. Activity was not regained through exposure of the poisoned catalyst to flowing O_2 as an attempt to remove sulfur on the catalyst surface through oxidation.

Discussion

Mechanism. The observation of the lead−lag of the adsorbed species and product formation has led to the following proposed mechanism:

$$CH_4 + (5 - x)^* \rightarrow {}^*CH_x + (4 - x)^*H \quad (1a)$$

$${}^*CH_x + (4 - x)^*H \leftrightarrow {}^*C + 4^*H \quad (1b)$$

$$CH_4 + {}^*O + (4 - x)^* \leftrightarrow {}^*CH_xO + (4 - x)^*H \quad (2)$$

$${}^*CH_xO + {}^* \leftrightarrow + {}^*OH + {}^*CH_x \quad (3)$$

$$2^*H \leftrightarrow H_2 + 2^* \quad (4)$$

$${}^*H + CO_2 \leftrightarrow {}^*OH + {}^*CO \quad (5)$$

$$CO_2 + 2^* \leftrightarrow {}^*CO + {}^*O \quad (6)$$

$${}^*C + {}^*O \leftrightarrow {}^*CO + {}^* \quad (7)$$

$${}^*H + {}^*O \leftrightarrow {}^*OH + {}^* \quad (8)$$

$${}^*OH + {}^*H \leftrightarrow H_2O + 2^* \quad (9)$$

$${}^*CO \leftrightarrow CO + {}^* \quad (10)$$

where "*" indicates an adsorption site of the catalyst and "*x*" is an integer such that $0 \leq x \leq 3$.

The proposed mechanism consists of a sequence of C−H/C−O bond breaking and H−H/C−O bond formation steps. The fundamental questions to be addressed pertain to the sequence of the reaction steps and the rate-limiting step: What is the first step of the reaction? What is the rate-limiting step which controls the rate of the overall reaction process? The first step of the overall reaction sequence can be revealed by examining the lead−lag relationship in the transient H_2 and CO product formation profiles. Figure 5 shows that H_2 formation leads that of CO during the CH_4 pulse into flowing CO_2, indicating that the formation of H_2 is a facile step upon CH_4 decomposition. It is very likely that methane decomposition is the first step to produce H_2 as represented by step 1a. CH_x formed from step 1a may further decompose to surface carbon and hydrogen, as shown in step 1b.

The *x* value in step 1 has been determined by the pulse surface reaction rate analysis (PSRA) over Ni catalysts;[34] the *x* value is in the range of 1.0−2.7 on Ni with varying supports. PSRA study of our Rh/Al_2O_3 catalyst gave identical profiles for both CO and H_2, suggesting that *x* approaches 0. This is consistent with the lack of observed C−H vibrations and CHO species via IR analysis. It has been concluded that CH_x is a minor reaction intermediate on Rh/Al_2O_3.[2] It should be noted that the concentration of a species on the surface depends on its formation and conversion rates. The importance of a surface species in a catalytic cycle cannot be simply determined by its surface concentration (i.e., coverage).

The adsorbed H species produced in step 1 can further react with CO_2, which can lead to the formation of linear CO and OH as illustrated in step 5. The proposed step 5 is also consistent with the observation of the emergence of the linear CO species upon pulsing CH_4 into CO_2 in Figure 5. The possibility of this step is further supported by the fact H_2 is formed prior to formation of CO (in Figures 4 and 6) and an abundant amount of *H and H_2 formed from CH_4 is available for the activation of CO_2 for its dissociation. H-assisted CO_2 dissociation has also been proposed in both the CO_2-CH_4 reaction[11,35] and CO_2 hydrogenation.[36]

The presence of linear CO on the Rh surface during the CH_4-CO_2 reforming reaction, the O_2 pulse into CO_2/CH_4, and the CH_4 pulse into CO_2 indicates that (i) linear CO accumulates on the Rh surface and (ii) the Rh is in the reduced Rh^0 state which chemisorbs CO as linear CO. The absence of Rh^+-CO at 2100−2150 cm^{-1} and/or gem dicarbonyl at 2031 and 2101 cm^{-1} (which is stable in an oxidizing environment up to 773 K[37]) indicates that the Rh catalyst prefers to remain in a reduced state during the CO_2-CH_4 reaction and the O_2 pulse into CO_2/CH_4. The importance of the Rh^0 site for the CO_2-CH_4 reaction is further evidenced by a support effect study which shows that the activity of support Rh catalysts is strongly correlated with the surface concentration of Rh^0 site.[7]

The absence of Rh^+ during the CO_2-CH_4 reaction and the O_2 pulse into CO_2/CH_4 could be due to facile formation of adsorbed H or H_2 from CH_4 which kept the Rh surface in a reduced state, thus avoiding the formation of an oxygen island even in the presence of the O_2 pulse. As described in the Results section, the O_2 pulse in Figure 8 shows that the O_2 pulse reaction can be divided into two stages. Stage I is dominated by CH_4 oxidation (i.e., combustion) to CO_2 and H_2O; stage II is dominated by the enhanced CO_2-CH_4 reaction. The extent of CH_4 combustion decreased while that of the CO_2-CH_4 reaction increased with the number of repeated O_2 pulses.

Although we are not able to distinguish the difference in the nature of adsorbed oxygen and the active site between CH_4 combustion and the enhanced CO_2-CH_4 reaction, it is instructive to compare the results of the first and fifth O_2 pulses as well as those of combustion/partial oxidation of CH_4 reported in the literature. It has been recognized that high surface concentration of adsorbed oxygen is responsible for CH_4 combustion while the low surface concentration of adsorbed O^{2-} is responsible for activation of CH_4 for partial oxidation.[38,39] Studies by Qin et al. further revealed that strongly bonded oxygen activates partial oxidation while weakly bonded oxygen is highly reactive for combustion.[40] It has also been shown that Rh is an effective catalyst for the partial oxidation of CH_4 to CO/H_2.[41] The high activity of Rh for partial oxidation reflects its ability to produce weakly bonded oxygen.

As the number of oxygen pulses increased (Figure 6), total oxidation (i.e., formation of CO_2 and H_2O) decreased, while

CO and H_2 formation amounts increased with each subsequent O_2 pulse. Repeated runs confirmed this observation, demonstrating its reproducibility. As the number of O_2 pulses increased, the Rh surface was modified. The nature of adsorbed oxygen and its concentration may shift from a high concentration of weakly adsorbed oxygen to a low concentration of strongly adsorbed oxygen, which is highly active for methane activation. Activation of CH_4 (step 1), $CH_4 + (5 - x)^* \rightarrow CH_x + (4 - x)^*H$, has been proposed to be the rate-limiting step of the CO_2-CH_4 reaction.[2,13] Our results also support this step as rate-limiting: (i) adsorbed CH_x, an IR-active species, was not observed during any of the experiments over Rh/Al_2O_3, and (ii) the activation energy of CH_4 conversion (16 kcal/mol) was determined to be higher than that of CO_2 conversion as well as CO formation (9 and 12 kcal/mol, respectively). The lack of IR bands corresponding to adsorbed CH_x suggests that the rate of conversion of $^*CH_x$ is greater than its rate of formation.

Our observation of enhanced CO and H_2 formation following the O_2 pulse suggests that an enhancement of CH_4 activation can be achieved by the strongly adsorbed oxygen via step 2, $CH_4 + ^*O + (4 - x)^* \Leftrightarrow ^*CH_xO + (4 - x)^*H$, and step 3, $^*CH_xO + ^* \Leftrightarrow ^*OH + ^*CH_x$. $^*CH_xO$ has been postulated to be an important reaction intermediate.[42] This species was not detected by our in situ IR technique, possibly due to its high rate of decomposition, i.e., step 3, under reaction conditions. The $^*CH_xO$ species may breakdown into either (i) *CO and H_2 or (ii) *OH and $^*CH_x$. The former is a route for partial oxidation of CH_4; the latter, i.e., step 3, produces *OH and $^*CH_x$ which can enter the CO_2-CH_4 reaction pathway to increase H_2 and CO formation. This latter step is supported by our observation of increased *OH, shown in Figure 8, and the stoichiometric ratio of near 1:1 for increased H_2/CO formation. The O_2 pulse resulted in a decrease in the *OH vibration, which was subsequently replenished in a rapid fashion. We speculate that the initial decrease in *OH vibration is due to localized heating of the surface upon exposure to O_2 (exothermic); the *OH is removed in the form of H_2O.

Conclusion

In situ IR study combined with mass spectrometric analysis of pulsing CH_4 into CO_2 flow and step switching from He to CO_2/CH_4 flow showed that the formation of H_2 led that of linear and gaseous CO. This observation revealed that the first step of the reaction sequence is the decomposition of CH_4 into $^*CH_x$ species and hydrogen. Hydrogen can assist in the activation of CO_2 to produce linear CO species. In situ infrared study shows that the CO_2-CH_4 reaction produced linear CO as a major adsorbate on Rh/Al_2O_3 in a temperature range of 673−873 K. Steady-state isotopic $^{13}CO_2$ transient studies at 773 K and 0.1 MPa showed that linear CO is an active adsorbate with a coverage of 0.112, which depends on the concurrent rates of its formation, conversion, and desorption. The observation of linear CO on the Rh^0 site during the pulse, step, and steady-state studies revealed that (i) the surface of Rh crystallites on Al_2O_3 remained in a reduced state throughout these studies and (ii) CO formed from the reaction accumulates on the Rh^0 surface as linear CO. Pulsing O_2 into CO_2/CH_4 produced two types of oxygen species: the first type completely oxidized CH_4 to CO_2 and H_2O and the second type enhanced the formation of CO and H_2. Activation of CH_4 was proposed as rate-limiting. Development of a selective poisoning approach to inhibit complete CH_4 oxidation would enhance CO/H_2 formation from the mixed reforming reaction, i.e., combined CO_2-CH_4 and CH_4 partial oxidation reactions.

Acknowledgment. This work was partially financed by the Ohio Board of Regents Grant R4552-OBR.

References and Notes

(1) Davis, B. H. *Catal. Today* **2003**, *84*, 83.
(2) Erdohelyi, A.; Cserenyi, J.; Solymosi, F. *J. Catal.* **1993**, *141*, 287.
(3) Efstathiou, A. M.; Kladi, A.; Tsipouriari, V. A.; Verykios, X. E. *J. Catal.* **1996**, *158*, 64.
(4) Basini, L.; Sanfilippo, D. *J. Catal.* **1995**, *157*, 162.
(5) Richardson, J. T.; Paripatyadar, S. A. *Appl. Catal.* **1990**, *61*, 293.
(6) Wang, H. Y.; Ruckenstein, E. *Appl. Catal., A: Gen.* **2000**, *204*, 143.
(7) Yokota, S.; Okumura, K.; Niwa, M. *Catal. Lett.* **2002**, *84*, 131.
(8) Portugal, U. L.; Santos, A. C. S. F.; Damyanova, S.; Marques, C. M. P.; Bueno, J. M. C. *J. Mol. Catal. A: Chem.* **2002**, *184*, 311.
(9) Basile, F.; Fornasari, G.; Trifiro, F.; Vaccari, A. *Catal. Today* **2002**, *77*, 215.
(10) Prabhu, A. K.; Oyama, S. T. *J. Membr. Sci.* **2000**, *176*, 233.
(11) Bradford, M. C. J.; Vannice, M. A. *J. Catal.* **1999**, *183*, 69.
(12) Erdohelyi, A.; Cserenyi, J.; Papp, E.; Solymosi, F. *Appl. Catal., A* **1994**, *108*, 205.
(13) Rostrup-Nielsen, J. R.; Bak Hansen, J. H. *J. Catal.* **1993**, *144*, 38.
(14) O'Connor, A. M.; Ross, J. R. H. *Catal. Today* **1998**, *46*, 203.
(15) Wolf, D.; Barre-Chassonnery, M.; Hohenberger, M.; van Veen, A.; Baerns, M. *Catal. Today* **1998**, *40*, 147.
(16) Ruckenstein, E.; Hu, Y. H. *Appl. Catal., A: Gen.* **1999**, *183*, 85.
(17) Zhang, Z. L.; Verykios, X. E. *Catal. Today* **1994**, *21*, 589.
(18) Tang, S. B.; Qiu, F. L.; Lu, S. J. *Catal. Today* **1995**, *24*, 253.
(19) http://chemacx.cambridgesoft.com, July 23, 2003.
(20) Bradford, M. C. J.; Vannice, M. A. *Catal. Rev.—Sci. Eng.* **1999**, *41*, 1.
(21) Lercher, J. A.; Bitter, J. H.; Hally, W.; Niessen, W.; Seshan, K. *Stud. Surf. Sci. Catal.* **1996**, *101*, 463.
(22) Chuang, S. S. C.; Brundage, M. A.; Balakos, M. W.; Srinivas, G. *Appl. Spectrosc.* **1995**, *49*, 1151.
(23) Yates, J. T., Jr.; Cavanagh, R. R. *J. Catal.* **1982**, *74*, 97.
(24) Stoop, F.; Toolenaar, F. J. C. M.; Ponec, V. *J. Catal.* **1982**, *70*, 50.
(25) Chuang, S. S. C.; Pien, S. I. *J. Catal.* **1992**, *135*, 618.
(26) Tamaru, K. Transient Catalytic Studies. In *Handbook of Heterogeneous Catalysis*; Ertl, G., Knozinger, H., Weitekamp, J., Eds.; Wiley-VCH: Weinheim, 1997; Vol. 3; p 1012.
(27) Shannon, S. L.; Goodwin, J. G., Jr. *Chem. Rev.* **1995**, *95*, 677.
(28) Balakos, M. W.; Chuang, S. S. C.; Srivivas, G. *J. Catal.* **1993**, *140*, 281.
(29) Srinivas, G.; Chuang, S. S. C.; Balakos, M. W. *AIChE J.* **1993**, *39*, 530.
(30) Stevens, R. W., Jr. Ph.D. Preliminary Study, The University of Akron, 2003.
(31) Biloen, P. *J. Mol. Catal.* **1983**, *21*, 17.
(32) Balakos, M. W.; Chuang, S. S. C. *J. Catal.* **1995**, *151*, 266.
(33) Levenspiel, O. *Chemical reaction engineering*, 3rd ed.; Wiley: New York, 1999.
(34) Osaki, T.; Masuda, H.; Mori, T. *Catal. Lett.* **1994**, *29*, 33.
(35) Luo, J. Z.; Yu, Z. L.; Ng, C. F.; Au, C. T. *J. Catal.* **2000**, *194*, 198.
(36) Behr, A. Activation of Carbon Dioxide Via Coordination To Transition Metal Complexes. In *Catalysis in C1 Chemistry*; Keim, W., Ed.; D. Reiedel Publishing Co.: Boston, 1983; p 169.
(37) Chuang, S. S. C.; Tan, C. D. *J. Catal.* **1998**, *173*, 95.
(38) Weng, W. Z.; Yan, Q. G.; Luo, C. R.; Liao, Y. Y.; Wan, H. L. *Catal. Lett.* **2001**, *74*, 37.
(39) Wang, D.; Dewaele, O.; De Groote, A. M.; Froment, G. F. *J. Catal.* **1996**, *159*, 418.
(40) Qin, D.; Lapszewicz, J.; Jiang, X. *J. Catal.* **1996**, *159*, 140.
(41) Witt, P. M.; Schmidt, L. D. *J. Catal.* **1996**, *163*, 465.
(42) Bradford, M. C. J.; Vannice, M. A. *Appl. Catal., A* **1996**, *142*, 73.